*Journal of Fluorine Chemistry, 51* (1991) 305–322



Received: November 8, 1989; accepted: December 6, 1990

# INSTANT LIGANDS, PART 6 [1]. STRUCTURES OF GASEOUS $(F_2P)S(CH_2)_3S(PF_2)$ AND $(F_2P)SEt$ BY ELECTRON DIFFRACTION: PREPARATION OF $[RuCl_2(p\text{-cymene})]_2[\mu\text{-}(F_2P)Y(CH_2)_nY(PF_2)]$ (Y = O, S; $n$ = 3–6) AND STRUCTURE OF $[RuCl_2(p\text{-cymene})]_2[\mu\text{-}(F_2P)O(CH_2)_4O(PF_2)]$ BY X-RAY CRYSTALLOGRAPHY

GRAEME A. BELL, ALEXANDER J. BLAKE, ROBERT O. GOULD AND DAVID W.H. RANKIN*

*Department of Chemistry, University of Edinburgh, West Mains Road, Edinburgh, EH9 3JJ (U.K.)*

## SUMMARY

The molecular structures of $(F_2P)SEt$ and $(F_2P)S(CH_2)_3S(PF_2)$ in the gas phase have been determined by electron diffraction. In both compounds the conformation adopted involves close contacts (ca. 260 pm) between fluorine atoms and hydrogen atoms of the adjacent $CH_2$ groups. Principal parameters ($r_a$, with the value for $(F_2P)SEt$ given first in each case) are: $r$(P–S) 208.5(3), 211.7(6), $r$(P–F) 158.7(4), 157.7(4), $r$(S–C) 182.5(6), 184.4(9) pm, <FPF 96.2(4), 99.1(14) and <FPS 101.1(2), 101.1(5)°. In $(F_2P)SEt$ the angles PSC and SCC refined to 100.3(6) and 108.4(9)° respectively, but they were not refined in the other case.

The compounds $(F_2P)Y(CH_2)_nY(PF_2)$ (Y = O, S; $n$ = 3–6) reacted with $[RuCl_2(p\text{-cymene})]_2$ to give $[RuCl_2(p\text{-cymene})]_2[\mu\text{-}(F_2P)Y(CH_2)_nY(PF_2)]$. These complexes were then characterised by n.m.r. spectroscopy, and the case of Y = O, $n$ = 4, by single-crystal X-ray crystallography.

0022-1139/91/$3.50 

## INTRODUCTION

Since the discovery [2] of the general reaction

$$S(PF_2)_2 + RYH \longrightarrow RYPF_2 + PF_2HS \quad (1)$$

we have used this route to prepare a wide range of fluorophosphine ligands. The preparation and properties of bidentate ligands derived from straight-chain substrates $HY(CH_2)_nYH$ (Y = O, S; $n$ = 2–12) have been described [3], and ligands prepared from dihydroxy aromatic compounds have been characterised: [4]. Structures of these compounds, both uncomplexed and when bound to metals, are important, as they provide information which can be used to help select organic substrates which will give multidentate ligands having predictable binding characteristics. Some derivatives of dihydroxybenzenes have already been studied [5], and in this paper we turn our attention to fluorophosphines made from straight-chain organic thiols, dithiols and diols. We report the structure in the gas phase of $(F_2P)S(CH_2)_3S(PF_2)$, which is expected to be the simplest of these bidentate ligands for structural study, and $(F_2P)SCH_2CH_3$ has also been investigated, as this is a more straightforward system, and so can provide useful data for comparison.

Solid-state data have been harder to come by, as the flexibility of the chains leads to the formation of glasses. Although a whole series of molybdenum pentacarbonyl complexes of these bidentate ligands has been prepared [3], none of them could be crystallised. We have therefore made further studies of the reactions of the ligands, with $[RuCl_2(p\text{-cymene})]_2$, and prepared a new series of complexes, of general formula $[RuCl_2(p\text{-cymene})]_2[\mu\text{-}(F_2P)Y(CH_2)_nY(PF_2)]$ (Y = O, S; $n$ = 3–6). However, the only one of these new compounds which has given single crystals even of a very poor quality is $[RuCl_2(p\text{-cymene})]_2[\mu\text{-}(F_2P)O(CH_2)_4O(PF_2)]$. In this case disorder in the chain of methylene groups has further limited the precision of the results. Nevertheless, important conformational differences between the gaseous sulphur compound and the crystalline oxygen compound have been observed.

## EXPERIMENTAL

Samples of $(F_2P)SEt$ and $(F_2P)S(CH_2)_3S(PF_2)$ were prepared by the reactions of ethanethiol and propan-1,3-dithiol respectively with excess $S(PF_2)_2$ [3]. They were purified by fractional condensation in a Pyrex glass vacuum line, and their purities were checked by i.r. and n.m.r. spectroscopy. Other fluorophosphine ligands were prepared by similar methods [3], and $[RuCl_2(p\text{-cymene})]$ was synthesised by dehydrogenation of 5-isopropyl-2-methyl-cyclohexa-1,3-diene with ethanolic ruthenium(III) trichloride [6].

The complexes $[RuCl_2(p\text{-cymene})]_2[\mu\text{-}(F_2P)S(CH_2)_nS(PF_2)]$ ($n$ = 3-6) were prepared in n.m.r. tubes by mixing 0.05 mmol of the ligand with a solution of 0.1 mmol of $[RuCl_2(p\text{-cymene})]_2$ dissolved in 0.5 ml $CCl_3D$ at low temperature and warming the solution to room temperature for 10 minutes. The $^{31}P$ and $^{19}F$ spectra were recorded, giving the parameters listed in Table 1, but the complexes decomposed before $^{13}C$ spectra could be recorded, and no attempts were made to isolate the products.

The analogous complexes containing oxygen instead of sulphur, $[RuCl_2(p\text{-cymene})]_2[\mu\text{-}(F_2P)O(CH_2)_nO(PF_2)]$ ($n$ = 3-6), were also prepared in n.m.r. tubes, using 0.05 mmol of the ligand and 0.05 mmol of the ruthenium complex in 0.5 ml of $CCl_3D$. The reactions were conducted at room temperature and were complete in 10 minutes, giving product mixtures each containing two components, unreacted $[RuCl_2(p\text{-cymene})]_2$ and the desired product. The components were separated using a column packed with activated silica and $CCl_2H_2$ as eluant. The faster-eluting orange band was identified as the starting complex and the slower-eluting yellow band as the fluorophosphine complex. Yields were *ca.* 20% for $n$ = 3, 5 and 6, but for $n$ = 4 the yield was *ca.* 40%. Crystals of this compound were grown by treating a $CCl_2H_2$ solution of the complex with 60-80 petroleum ether.

TABLE 1

N.m.r. parameters for $[RuCl_2(p\text{-cymene})]_2[\mu\text{-}(F_2P)Y(CH_2)_nY(PF_2)]$

| Y = | O | O | O | O | S | S | S | S |
|---|---|---|---|---|---|---|---|---|
| *n* = | 3 | 4 | 5 | 6 | 3 | 4 | 5 | 6 |
| $\delta\ ^{31}P$ | 115.6 | 115.0 | 115.8 | 117.0 | 196.6 | 196.9 | 197.0 | 197.1 |
| $\delta\ ^{19}F$ | -33.6 | -33.6 | -35.0 | -36.5 | -40.4 | -40.1 | -41.6 | -41.8 |
| $^1J(PF)$ | 1292 | 1292 | 1293 | 1294 | 1245 | 1244 | 1245 | 1245 |
| $\delta\ ^1H_a$ | 2.16 | 2.18 | 2.17 | 2.18 | | | | |
| $\delta\ ^1H_b$ | 1.20 | 1.21 | 1.20 | 1.19 | | | | |
| $\delta\ ^1H_c$ | 2.82 | 2.82 | 2.83 | 2.82 | | | | |
| $\delta\ ^1H_d$ | 5.84 | 5.81 | 5.83 | 5.83 | | | | |
| $\delta\ ^1H_e$ | 5.59 | 5.55 | 5.58 | 5.57 | | | | |
| $^3J(H_aH_b)$ | 6.9 | 6.9 | 6.9 | 6.8 | | | | |
| $^3J(H_dH_e)$ | 6.4 | 6.4 | 6.4 | 6.4 | | | | |

Spectra recorded for solutions in $CCl_2D_2$ at 300 K.

$H_a$ represents protons of the unique methyl group of p-cymene, $H_b$ and $H_c$ the ring protons *ortho* and *meta* to the methyl group, and $H_d$ and $H_e$ the methinyl and methyl protons of the iso-propyl group.

*Electron diffraction*

Electron diffraction scattering intensities were recorded on Kodak Electron Image photographic plates using the Edinburgh gas diffraction apparatus [7], operating at *ca.* 44.5 kV. Three or four plates were recorded for each compound at each of the two camera distances (*ca.* 128 and 285 mm), and in every experiment the samples and nozzle were maintained at room temperature, *ca.* 295 K. Optical densities of plates were obtained in digital form using a Joyce-Loebl MDM6 microdensitometer [8] at the S.E.R.C. Laboratory, Daresbury. The programs used to control the scanner [8], for data reduction [8] and for least-squares analysis [9] have all been described previously. Standard scattering factors [10] were used in all calculations.

In Table 2 details are given of the *s* ranges of the data, and weighting points used in setting up the off-diagonal weight matrices used in the least-squares refinements. The electron wavelengths and camera distances

TABLE 2

Weighting functions, correlation parameters and scale factors

| Compound | Camera height (mm) | $\Delta s$ | $s_{min}$ | $sw_1$ | $sw_2$ | $s_{max}$ ($nm^{-1}$) | Correlation parameter | Scale factor | Wavelength (pm) |
|---|---|---|---|---|---|---|---|---|---|
| $(F_2P)SEt$ | 128.39 | 4 | 6 | 8 | 25 | 30 | -0.19 | 0.694(18) | 5.702 |
| | 285.28 | 2 | 2 | 4 | 12 | 14 | 0.34 | 0.721(15) | 5.701 |
| $(F_2P)S(CH_2)_3S(PF_2)$ | 128.35 | 4 | 7 | 9 | 25 | 29 | -0.31 | 0.314(7) | 5.700 |
| | 285.50 | 2 | 2 | 4 | 12 | 14 | 0.33 | 0.441(4) | 5.700 |

which are also given in this table were determined by analysis of scattering patterns for benzene, recorded on the same occasions as the plates for the fluorophosphines were exposed. These plates were analysed in the same way as those for the compounds being studied, and so systematic errors are minimised. Errors in wavelengths and camera distances do not make any significant contribution to the overall errors in geometrical parameters.

*X-ray diffraction*

Preliminary photography showed that even the best of the available crystals of $[RuCl_2(p\text{-cymene})]_2[\mu\text{-}(F_2P)O(CH_2)_4O(PF_2)]$ were of poor quality: very few reflections were visible at higher $2\theta$ angles and those at low angle were very broad. Nevertheless, this crystal was mounted in a capillary tube and set to rotate about c on a Stoë STADI-2 two-circle diffractometer.

*Crystal Data*: $C_{24}H_{36}Cl_4F_4O_2P_2Ru_2$, $M$ = 838.7, trigonal, space group *R3*, $a$ = 23.159(13), $c$ = 19.522(6) A, $V$ = 9068 $A^3$ [from setting angles for 13 reflections with $2\theta$ = 6-18°, $\lambda$ = 0.71073 A], $Z$ = 9, $D_{calc}$ = 1.382 g $cm^{-3}$, $T$ = 293 K, red column, 0.60 x 0.125 x 0.075 mm, $\mu$ = 1.073 $mm^{-1}$, $F(000)$ = 3762.

*Data Collection and Processing*: STADI-2 diffractometer with graphite-monochromated Mo-$K_\alpha$ $X$-radiation, $T$ = 293 K, $\omega$ scans with width [5.0 + 2.5(sin$\mu$/tan$\theta$)]°, 1920 reflections measured ($2\theta_{max}$ 40°, $h$ -22 → 22, $k$ 0

→ 22, $l$ 0 → 18), 1839 unique ($R_{int}$ 0.017), giving 471 with $F \geq 6\sigma(F)$ for use in all calculations. No significant crystal decay or movement, no absorption correction.

## STRUCTURE ANALYSIS

### *Electron diffraction*

*Molecular models*: The structure of $(F_2P)SEt$ was described by a model in which local $C_s$ symmetry was assumed for the $SPF_2$ and $SCH_2C$ units, while the $CCH_3$ group had local $C_{3v}$ symmetry. The $SCH_2CH_3$ fragment was also assumed to adopt a perfectly staggered conformation. The C–H bonds in methyl and methylene groups were assumed to be of equal length. The geometry was then defined by five different bonded distances, six valence angles, and torsion angles about the P–S and S–C bonds, as listed in Table 3. The first of these torsion angles was defined to be zero when the bisector of the FPF angles was *syn* to the S–C bond, while the S–C torsion angle was taken to be zero for an *anti* C–C–S–P arrangement. For $(F_2P)S(CH_2)_3S(PF_2)$ a similar set of parameters sufficed, with the addition of a CCC angle at the central carbon atom. Here the three methylene groups were assumed to be identical and the two ends of the molecule were constrained to adopt equivalent conformations. The torsion angle about the C–C bonds was no longer forced to correspond to a staggered arrangement, which was defined as the zero position for an extra variable. Altogether, therefore, there were fifteen parameters which could in principle be refined for this molecule, and these are listed in Table 3.

*Refinement of $(F_2P)SEt$ structure*: The radial distribution curve for $(F_2P)SEt$ (Fig. 1) shows four clear peaks in the region of bonded distances, and only the C–C and P–F peaks overlap. It proved to be possible to refine four distances and their associated amplitudes of vibration, and the C–C distance was fixed at 153 pm. All four valence angles which did not involve hydrogen were also easily refined, although it was necessary to constrain three vibrational

TABLE 3

Geometrical parameters

| | Parameter[a] | $(F_2P)SEt$ | $(F_2P)S(CH_2)_3S(PF_2)$ |
|---|---|---|---|
| $p_1$ | r(P-F) | 158.7(2) | 157.7(4) |
| $p_2$ | r(P-S) | 208.5(3) | 211.7(6) |
| $p_3$ | r(S-C) | 182.5(6) | 184.4(9) |
| $p_4$ | r(C-C) | 153.0[b] | 153.0[b] |
| $p_5$ | r(C-H) | 113.6(7) | 108.6[b] |
| $p_6$ | <FPF | 96.2(4) | 99.1(14) |
| $p_7$ | <FPS | 101.1(2) | 101.1(5) |
| $p_8$ | <PSC | 100.3(6) | 100.0[b] |
| $p_9$ | <SCC | 108.4(9) | 108.4[b] |
| $p_{10}$ | <CCC | | 109.0[b] |
| $p_{11}$ | <CCH | 109.5[b] | 109.5[b] |
| $p_{12}$ | <HCH | 108.0[b] | 108.0[b] |
| $p_{13}$ | P-S torsion | -8.9(34) | -31.1(35) |
| $p_{14}$ | S-C torsion | 95.7(40) | 85.1(22) |
| $p_{15}$ | C-C torsion | 0.0[b] | -142.6(29) |

[a] Distance in pm, angles in degrees

[b] Fixed

amplitudes to be equal to one another. This then left the conformation to be determined. At first a series of refinements was performed, with the torsion angles about the P–S and S–C bonds being stepped systematically at 15° intervals so that the whole possible range of conformations was studied. This showed that the P–S torsion angle was close to zero, so that the fluorine atoms were close to C(5), while the S–C torsion angle was near 90°, thus placing one hydrogen atom of the $CH_2$ group close (*ca.* 260 pm) to both fluorine atoms, with one of the $CH_3$ hydrogens also close (*ca.* 245 pm) to one fluorine. The torsion angles were then allowed to refine from these values, and the set of parameters listed in Table 3 was obtained. The R factor ($R_G$) at this stage was 0.078. The most significant elements of the least-squares correlation

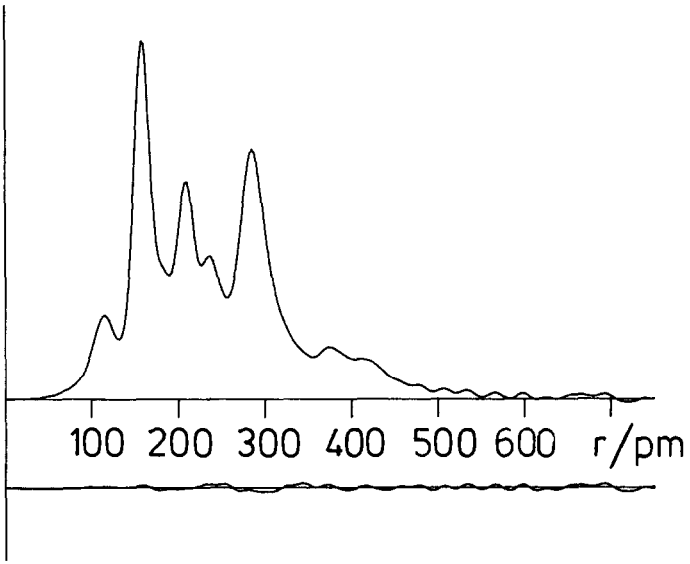


Fig. 1. Observed and final weighted difference radial distribution curves, $P(r)/r$, for $(F_2P)SEt$. Before Fourier inversion the data were multiplied by $s \cdot \exp(-0.00003s^2)/(Z_P - f_P)(Z_F - f_F)$.

TABLE 4

Least-squares correlation matrix for $(F_2P)SEt$ X 100[a]

| | $p_7$ | $p_{14}$ | $u_1$ | $u_3$ | $u_7$ | $k_1$ | $k_2$ |
|---|---|---|---|---|---|---|---|
| $p_1$ | | | | -51 | | | |
| $p_2$ | -53 | | | | | | |
| $p_3$ | | | 51 | | | | |
| $p_9$ | | | | | 64 | | |
| $p_{13}$ | | 83 | | | | | |
| $p_{14}$ | | -56 | | | | | |
| $u_1$ | | | | -55 | | 87 | 66 |
| $u_3$ | | | | | | -67 | -53 |
| $k_1$ | | | | | | | 68 |

[a] Only elements >50% are listed.

matrix are given in Table 4, and interatomic distances and amplitudes of vibration are listed in Table 5. Figure 2 shows the molecular scattering intensity curve and Fig. 3 is a perspective view of the molecule, showing the atomic numbering.

*Refinement of $(F_2P)S(CH_2)_3S(PF_2)$ structure*: This compound was known to be of limited stability at room temperature, and it became apparent at an early

TABLE 5

Interatomic distances ($r_a$/pm) and amplitudes of vibration (u/pm)

| | | $(F_2P)SEt$ | | $(F_2P)S(CH_2)_3S(PF_2)$ | |
|---|---|---|---|---|---|
| | | Distance | Amplitude | Distance | Amplitude |
| $r_1$ | P-F | 158.7(2) | 3.3(4) | 157.7(4) | 4.4(3) |
| $r_2$ | P-S | 208.5(3) | 5.1(3) | 211.7(6) | 4.4(7) |
| $r_3$ | S-C | 182.5(6) | 6.4(9) | 184.4(9) | 4.4[a] |
| $r_4$ | C-C | 153.0[a] | 3.3[b] | 153.0[a] | 4.4[a] |
| $r_5$ | C-H | 113.6(7) | 6.2(9) | 108.6[a] | 7.0[a] |
| $r_6$ | F(2)···F(3) | 236.3(6) | 4.7(9) | 240.0(18) | 6.5(7) |
| $r_7$ | S(4)···F(2) | 285.3(5) | | 287.8(8) | |
| $r_8$ | P(1)···C(5) | 300.6(11) | 5.6(10) | 304.0(10) | 8.1(13) |
| $r_9$ | S(4)···C(8) | 272.6(12) | | 274.3(9) | |
| $r_{10}$ | C(5)···C(13) | | | 249.1[a] | 7.0[a] |
| $r_{11}$ | F(2)···C(5) | 317.5(39) | 15.0[a] | 352.5(47) | 15.0[a] |
| $r_{12}$ | F(3)···C(5) | 296.0(24) | 15.0[a] | 281.5(23) | 13.8[a] |
| $r_{13}$ | P(1)···C(8) | 375.4(37) | 16.1(18) | 363.3(28) | 15.0[a] |
| $r_{14}$ | F(2)···C(8) | 428.5(27) | 12.8(24) | 453.7(48) | 12.9(39) |
| $r_{15}$ | F(3)···C(8) | 315.9(59) | 20.0[a] | 298.3(38) | 13.8[a] |
| $r_{16}$ | S(4)···S(12) | | | 548.2(18) | 15.7[a] |
| $r_{17}$ | P(1)···S(12) | | | 605.4(37) | 25.0[a] |
| $r_{18}$ | P(1)···P(9) | | | 707.4(59) | 25.0[a] |

Other long-range distances not listed here were also included in the refinements.

[a] Fixed

[b] Tied to $u_1$

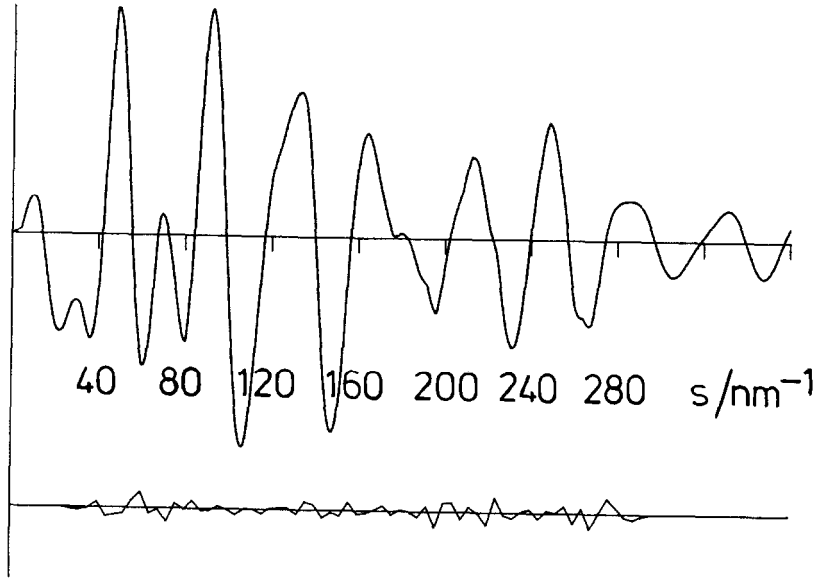


Fig. 2. Observed and final weighted difference combined molecular scattering intensity curves for $(F_2P)SEt$.

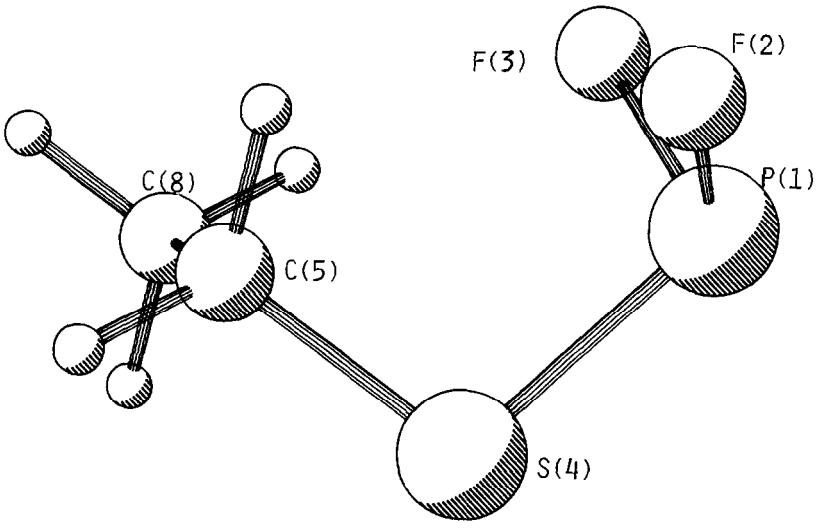


Fig. 3. A perspective view of $(F_2P)SEt$ showing the atom numbering scheme used.

stage of the structural analysis that the vapour passing through the nozzle must have contained a substantial proportion of $PF_3$. The radial distribution curve (Fig. 4) shows strong peaks at 155 and 235 pm, as well as many peaks associated with the compound being studied. In the analysis allowance was made for a variable amount of $PF_3$, which was assumed to have the published structure [11]. Ultimately the molar ratio of $PF_3$ to $(F_2P)S(CH_2)_3S(PF_2)$ refined to 1.68.

Refinement of the structure followed much the same pattern as that already described for $(F_2P)SEt$, except that the PSC, SCC and CCC angles all tended to refine downwards to unreasonable values, some 5 - 7° lower than expected, with little effect on the *R* factor. As the major purpose of the study was to investigate the conformation of the molecule, these angles were simply fixed at the values found earlier for $(F_2P)SEt$. The conformation was then studied by varying the C–C, S–C and P–S torsion angles in 15° steps over the whole

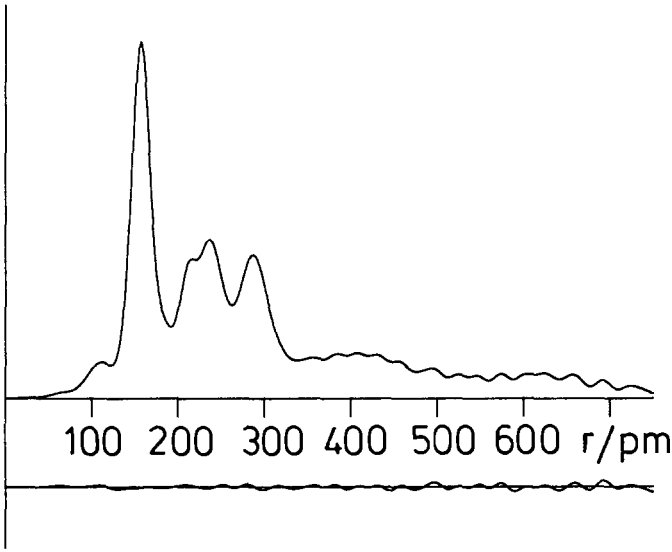


Fig. 4. Observed and final weighted difference radial distribution curves, $P(r)/r$, for $(F_2P)S(CH_2)_3S(PF_2)$. Before Fourier inversion the data were multiplied by $s \cdot \exp(-0.00003s^2)/(Z_P - f_P)(Z_F - f_F)$.

possible range, and it was soon found that the S–C and P–S torsion angles were close to those found for $(F_2P)SEt$. Note that it was assumed that the angles for the two ends of the molecules were the same, but that both $C_s$ and $C_2$ overall symmetries were considered. The C–C torsion angle was found to be about 30° away from the *anti* SCCC configuration, with overall $C_2$ symmetry. The three torsion angles were then added to the list of refining parameters, and the $R$ factor ($R_G$) went down to 0.104. The parameters, distances and amplitudes of vibration are given in Tables 3 and 5. The only element of the least-squares correlation matrix greater than 0.5 was between $u$(P–F) and the scale factor for the short camera distance data, at 0.76.

Figure 5 is a perspective view of the molecule, showing the atom numbering scheme, and Figure 6 shows the combined molecular intensity curve.

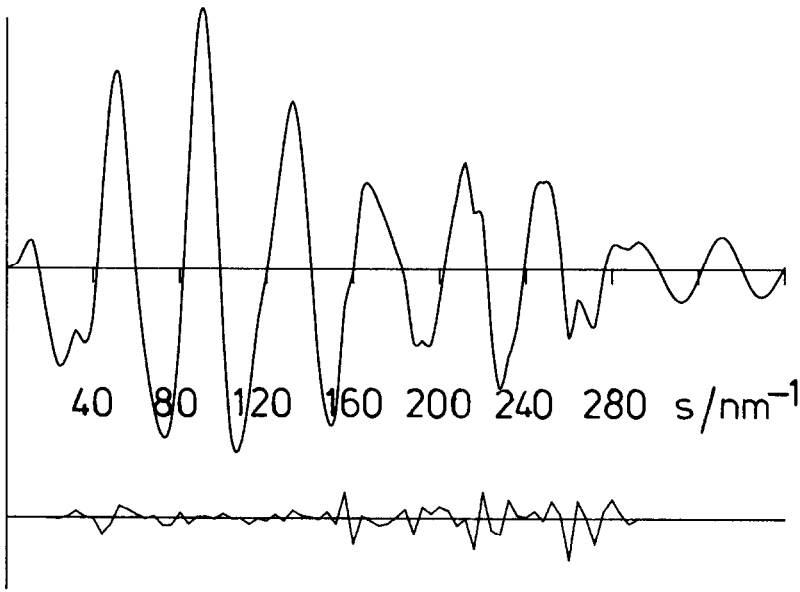


Fig. 5. Observed and final weighted difference combined molecular scattering intensity curves for $(F_2P)S(CH_2)_3S(PF_2)$.

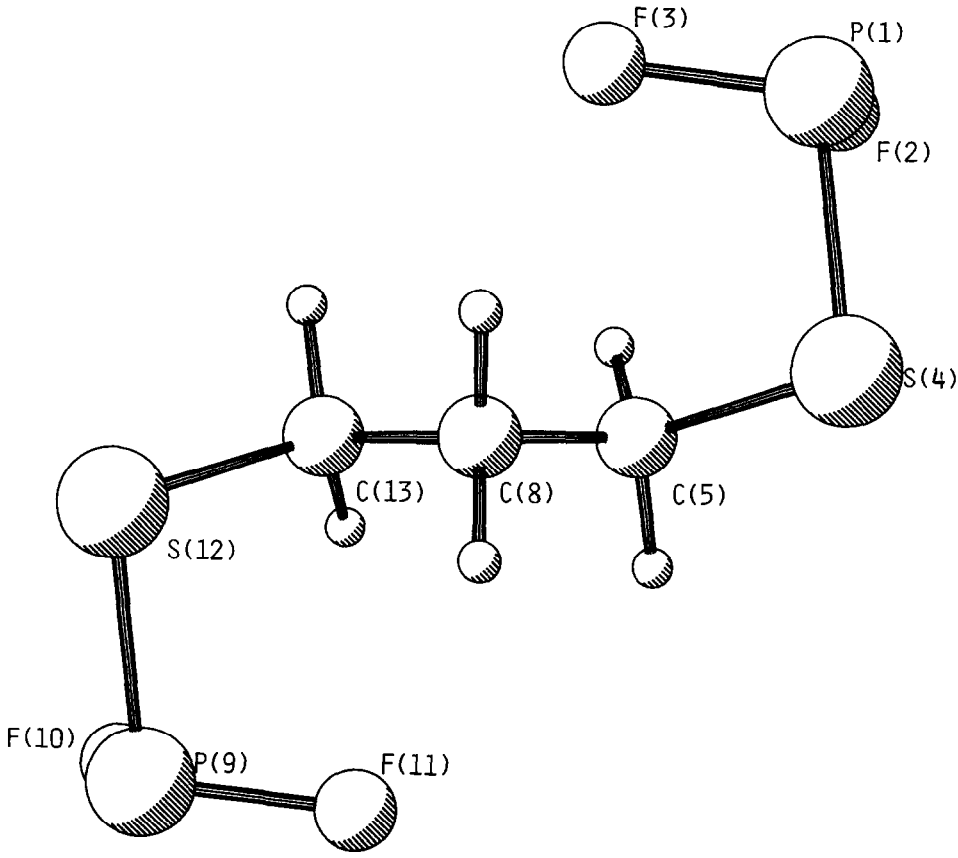


Fig. 6. A perspective view of $(F_2P)S(CH_2)_3S(PF_2)$ showing the atom numbering scheme used.

*X-ray Diffraction*

A Patterson synthesis located the Ru atom and subsequent iterative cycles of least-squares refinement and difference Fourier synthesis located all non-H atoms. These were then refined (by least-squares on *F* [12]) with anisotropic thermal parameters for Ru and Cl and with the phenyl ring of the p-cymene ligand constrained to be a rigid hexagon. Extensive disorder was found in the $-(CH_2)_4-$ chain, but this could be modelled to some extent by allowing it to adopt two orientations: in each of these the C atoms had 50% occupancy and a

fixed $U_{iso}$ of 0.08 $A^2$; the C–C and C–O bonds were held at 154 pm and angles at C were constrained to be tetrahedral. At final convergence $R$, $R_w$ = 0.0877, 0.1242 respectively, $S$ = 1.180 for 84 refined parameters and the final $\Delta F$ synthesis showed no peak above 0.77 e $A^{-3}$. The weighting scheme $W^{-1} = \sigma^2(F) + 0.0045F^2$ gave satisfactory agreement analyses and in the final cycle $(\Delta/\sigma)_{max}$ was 0.25. Atomic scattering factors were inlaid [12], or taken from Ref. [13]. Molecular geometry calculations utilised CALC [14] and Figure 7 was produced by ORTEPII [15]. Selected molecular geometric parameters and fractional atomic co-ordinates are given in Tables 6 and 7 respectively, while anisotropic thermal parameters and observed and calculated structure factors are available on request. Figure 7 shows the structure of the ruthenium complex in the crystal.

## DISCUSSION

The ligands $(F_2P)Y(CH_2)_nY(PF_2)$ (Y = O, S; $n$ = 3–6) all reacted rapidly with $[RuCl_2(p\text{-cymene})]_2$ to form complexes in which the bidentate ligand linked two ruthenium centres. Thermal instability of the complexes made elemental analysis impossible, but the identity of each product could be established from n.m.r. spectra. For sulphur-containing ligands, there was a reduction of $\delta^{31}P$ of *ca.* 39 ppm on complex formation, while $\delta^{19}F$ shifted by 28 ppm to higher frequency and $^1J(PF)$ decreased by *ca.* 70 Hz. These changes are in the directions normally associated with coordination of a fluorophosphine ligand. However, the $^{31}P$ chemical shifts and $^1J(PF)$ for the oxygen-containing ligands were almost unchanged when they formed complexes, and $\delta^{19}F$ increased by only 15 ppm. It was therefore not possible, on the basis of the n.m.r. data alone, to say how the ligands were coordinated to ruthenium. Indeed, the $^{31}P$ spectra provide no evidence for reaction at all. The unusually small changes in the n.m.r. parameters are nevertheless consistent with the structure determined subsequently by X-ray crystallography, with the ligands

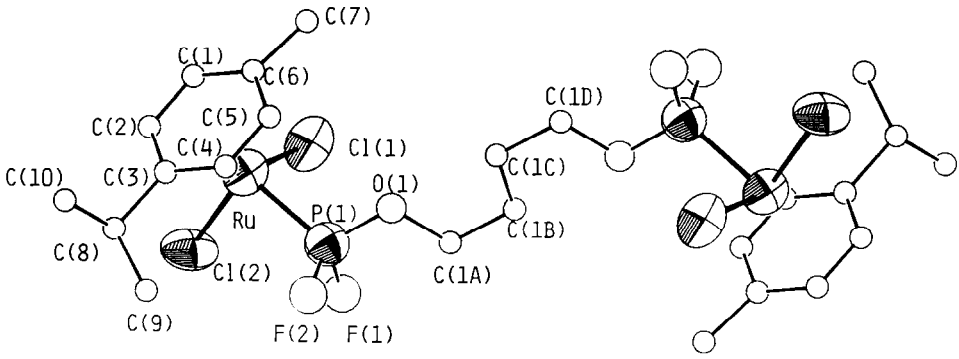


Fig. 7. A perspective view of the structure of $[RuCl_2(p\text{-cymene})]_2$-$[\mu\text{-}(F_2P)O(CH_2)_4O(PF_2)]$ in the crystal, showing the atom numbering adopted.

**TABLE 6**

**Selected bond lengths (pm), angles and torsions (degrees) in crystalline $[RuCl_2(p\text{-cymene})]_2[\mu\text{-}(F_2P)O(CH_2)_4O(PF_2)]$**

| | | | | | |
|---|---|---|---|---|---|
| Ru-Cl(1) | 238.5(20) | Ru-C(4) | 221(4) | P(1)-O(1) | 155(6) |
| Ru-Cl(2) | 240.6(20) | Ru-C(5) | 222(4) | O(1)-C(1A) | 154(9) |
| Ru-P(1) | 220(3) | Ru-C(6) | 224(4) | C(6)-C(7) | 152(7) |
| Ru-C(1) | 224(4) | P(1)-F(2) | 150(6) | C(8)-C(9) | 149(12) |
| Ru-C(2) | 223(4) | P(1)-F(2) | 161(5) | C(8)-C(10) | 145(13) |
| Ru-C(3) | 221(4) | | | | |
| Cl(1)-Ru-Cl(2) | 87.6(7) | | | F(2)-P(1)-O(1) | 109.3(33) |
| Cl(1)-Ru-P(1) | 82.4(9) | | | F(1)-P(1)-O(1) | 99.1(30) |
| Cl(2)-Ru-P(1) | 88.8(9) | | | P(1)-O(1)-C(1A) | 117.4(46) |
| Ru-P(1)-F(2) | 115.3(25) | | | C(1)-C(6)-C(7) | 124.3(40) |
| Ru-P(1)-F(1) | 119.7(22) | | | C(5)-C(6)-C(7) | 115.6(39) |
| Ru-P(1)-O(1) | 115.2(25) | | | C(9)-C(8)-C(10) | 112.6(76) |
| F(2)-P(1)-F(1) | 95.5(30) | | | | |
| F(2)-P(1)-O(1)-C(1A) | -57.4(57) | | C(4)-C(5)-C(6)-C(7) | | 176.7(41) |
| F(1)-P(1)-O(1)-C(1A) | 41.8(54) | | O(1)-C(1A)-C(1B)-C(1C) | | 28.3(74) |
| P(1)-O(1)-C(1A)-C(1B) | -170.1(46) | | C(1A)-C(1B)-C(1C)-C(1D) | | -167.1(56) |
| C(2)-C(1)-C(6)-C(7) | -176.4(43) | | | | |

TABLE 7

Atomic coordinates for $[RuCl_2(p\text{-cymene})]_2[\mu\text{-}(F_2P)O(CH_2)_4O(PF_2)]$

| | $x$ | $y$ | $z$ | $U_{iso}/Å^2$ |
|---|---|---|---|---|
| Ru | 0.7136(3) | 0.6495(3) | 0.21931(23) | 0.088(6) |
| Cl(1) | 0.7800(9) | 0.7584(9) | 0.1722(8) | 0.120(19) |
| Cl(2) | 0.6811(9) | 0.6097(9) | 0.1040(7) | 0.121(19) |
| P(1) | 0.6370(12) | 0.6792(12) | 0.2201(11) | 0.110(7) |
| F(2) | 0.567(3) | 0.6236(73) | 0.2306(23) | 0.173(18) |
| F(1) | 0.6215(21) | 0.7069(20) | 0.1512(22) | 0.161(17) |
| O(1) | 0.651(3) | 0.7376(23) | 0.269(3) | 0.172(21) |
| C(1) | 0.7994(14) | 0.6395(21) | 0.2573(19) | 0.052(16) |
| C(2) | 0.7502(14) | 0.5777(21) | 0.2326(19) | 0.089(21) |
| C(3) | 0.6853(14) | 0.5490(21) | 0.2579(19) | 0.087(20) |
| C(4) | 0.6696(14) | 0.5820(21) | 0.3079(19) | 0.066(18) |
| C(5) | 0.7189(14) | 0.6437(21) | 0.3325(19) | 0.073(17) |
| C(6) | 0.7838(14) | 0.6725(21) | 0.3072(19) | 0.091(21) |
| C(7) | 0.832(3) | 0.742(3) | 0.335(3) | 0.092(22) |
| C(8) | 0.627(4) | 0.481(4) | 0.219(4) | 0.13(3) |
| C(9) | 0.558(4) | 0.469(3) | 0.225(4) | 0.14(3) |
| C(10) | 0.638(4) | 0.436(5) | 0.262(5) | 0.20(4) |
| C(1A) | 0.605(3) | 0.767(3) | 0.264(4) | 0.0800 |
| C(1B) | 0.6341(23) | 0.832(3) | 0.307(3) | 0.0800 |
| C(1C) | 0.7105(20) | 0.864(3) | 0.310(4) | 0.0800 |
| C(1D) | 0.7380(10) | 0.919(4) | 0.366(4) | 0.0800 |

binding to ruthenium through the phosphorus atoms. It seems that when fluorophosphine ligands bind to $RuCl_2$(p-cymene), the changes in both $^{31}P$ and $^{19}F$ chemical shifts and in the P–F coupling constant are much smaller than usual and this effect is even more pronounced for binding to $Rh(C_5Me_5)Cl_2$. In some cases with the rhodium complexes $^1J(PF)$ *increases* on coordination, and $\delta^{31}P$ *decreases* [16].

TABLE 8

Structural parameters[a] for some difluorothiophosphines

| Compound | r(P-F) | r(P-S) | r(S-Y) | <FPF | <SPF | <PSY | Ref. |
|---|---|---|---|---|---|---|---|
| $S(PF_2)_2$ | 157.2(2) | 213.2(4) | | 97.4(5) | 100.2(4) | 91.3(11) | 17 |
| $(F_2P)SMe$ | 158.9(3) | 208.5(3) | 182.2(5) | 95.6(6) | 101.2(3) | 102.0(12) | 17 |
| $(F_2P)SEt$ | 158.7(2) | 208.5(3) | 182.5(6) | 96.2(4) | 101.1(2) | 100.3(6) | |
| $(F_2P)S(CH_2)_3S(PF_2)$ | 157.7(4) | 211.7(6) | 184.4(9) | 99.1(14) | 101.1(5) | 100.0[b] | |
| $(F_2P)SGeH_3$ | 159.0(9) | 211.5(8) | 225.6(4) | 97.0(10) | 99.9(4) | 99.0(6) | 18 |

[a] Distances in pm, angles in degrees

[b] Fixed

In Table 8 the major parameters for some compounds containing $(F_2P)S-$ groups are listed. Even in this fairly small group of structures there are variations of up to 2 pm in $r$(P–F), 5 pm in $r$(P–S) and 4° in the angles at phosphorus. Angles at sulphur are close to 100° when the sulphur atom is bound to carbon [17] or germanium [18] but can be as small as 91° in $S(PF_2)_2$ [17]. The widest angles at sulphur are associated with the shortest P–S bond distances.

The structure in the crystal comprises two $[RuCl_2(p\text{-cymene})]$ units linked through a bridging $(F_2P)O(CH_2)_4O(PF_2)$ ligand. The two halves of this molecule are related by a crystallographic inversion centre. The $-(CH_2)_4-$ chain is severely disordered, although we have been able to identify two major conformations.

## ACKNOWLEDGEMENTS

We thank the Science and Engineering Research Council for financial support and for the provision of microdensitometer facilities.

REFERENCES


1 Part 5, A.J. Blake, M.J. Davis and D.W.H. Rankin, *J. Mol. Struct.*, 221 (1990) 25.

2 E.R. Cromie, G. Hunter and D.W.H. Rankin, *Angew. Chem., Int. Ed. Engl.*, 19 (1980) 316.

3 G.A. Bell and D.W.H. Rankin, *J. Chem. Soc., Dalton Trans.*, (1986) 1689.

4 G.A. Bell, D.W.H. Rankin and P.F. Reinisch, *J. Chem. Soc., Dalton Trans.*, (1987) 3023.

5 G.A. Bell, D.W.H. Rankin and H.E. Robertson, *J. Mol. Struct.*, 178 (1988) 243.

6 M.A. Bennett and A.K. Smith, *J. Chem. Soc., Dalton Trans.*, (1974) 233.

7 C.M. Huntley, G.S. Laurenson and D.W.H. Rankin, *J. Chem. Soc., Dalton Trans.*, (1980) 954.

8 S. Cradock, J. Koprowski and D.W.H. Rankin, *J. Mol. Struct.*, 77 (1981) 113.

9 A.S.F. Boyd, G.S. Laurenson and D.W.H. Rankin, *J. Mol. Struct.*, 71 (1981) 217.

10 L. Schäfer, A.C. Yates and R.A. Bonham, *J. Chem. Phys.*, 55 (1971) 3055.

11 Y. Morino, K. Kuchitsu and T. Moritani, *Inorg. Chem.*, 8 (1969) 867.

12 SHELX76, program for crystal structure refinement. G.M. Sheldrick, University of Cambridge, (1976).

13 D.T. Cromer and J.L. Mann, *Acta Crystallogr., Sect. A.*, 24 (1986) 321.

14 CALC, program for molecular geometry calculations. R.O. Gould and P. Taylor, University of Edinburgh, (1985).

15 ORTEPII, interactive version. P.D. Mallinson and K.W. Muir, *J. Applied Cryst.*, 18 (1985) 51.

16 G.A. Bell and D.W.H. Rankin, Unpublished observations.

17 D.E.J. Arnold, G. Gundersen, D.W.H. Rankin and H.E. Robertson, *J. Chem. Soc., Dalton Trans.*, (1983) 1989.

18 E.A.V. Ebsworth, E.K. Macdonald and D.W.H. Rankin, *Monatsh.*, 111 (1980) 221.